PSO Based Controlled Six-phase Grid Connected Induction Generator for Wind Energy Generation

Arif Iqbal, *Member, IEEE*, and Girish Kumar Singh

***Abstract*— This paper deals a detailed performance investigation of asymmetrical six-phase grid connected induction generator (GCIG) in two proposed configurations in variable speed operation. During the system development, regulation of DC-link voltage has been proposed using particle swarm optimization (PSO) based PI controller, ensuring the power flow to utility grid through back to back converters. The closed loop operation of asymmetrical six-phase GCIG using indirect field oriented control in different configurations has been carried out in Matlab/Simulink environment. Analytical results have been verified using real time test results on virtual platform of Typhoon HIL supported with some experimental validation.**

***Index Terms*— Six-phase induction generator, particle swarm optimization (PSO), indirect field oriented control.**

I. INTRODUCTION

OWING to the limited availability of fossil fuel, a tremendous research activity is going on for last few decades to explore the various possibilities to generate renewable energy. This includes solar, wind, tidal, biomass etc. together with hybrid combination of these energy resources. It was noted that the wind power generation constitute a major role with the total installed capacity of 564 GW globally by 2018 [1] which is continuously increasing in annual market, particularly in Asian and European territories [2].

Power generation using wind is based on the conversion of turbine kinetic energy to electrical energy using AC machine as generator. Among the various option (asynchronous or synchronous machine), squirrel cage induction machine are particularly used due to various potential advantages, important of which is its robust operation, cost effective with reduced maintenance [3]. Usually, the generator employed in wind power generation is three-phase. But, multiphase (more than three-phase) machine has emerged as a preferable option for last few years due to the existence of various advantages with its three-phase counterpart. This includes the reduced effect of space and time harmonics, reduced per phase current with no change in terminal voltage enabling higher power transfer in same frame with higher reliability and higher degree of freedom [4]-[7]. Hence, multiphase machines are now preferably used in various applications, not limited to ship propulsion, electric vehicles, more electric aircraft, electric power generation etc. [8-9]. Also, six-phase induction machine may be easily realized by reconfiguring stator winding externally of existing three-phase machine with no additional expense [4, 10]. Six-phase induction machine (as generator) operates in two modes: (a) Standalone: where the locally connected loads are supplied through the power generated, (b) Grid connected: where generated electrical power is fed to utility grid. Six-phase induction generator in standalone mode has been investigated analytically and experimentally [11], [12] wherein capacitor bank is connected to the stator for excitation purpose during voltage buildup process. Capacitor selection procedure has been explained in [13]. Although the capacitor bank is connected in parallel with stator, but at higher load leads the deterioration in voltage regulation due to increased voltage drop in leakage reactance and resistance. This issue was proposed to be resolved by using series connection of capacitor with stator [14-16]. Generated voltage and frequency control in standalone mode using PWM converter supplying load has been discussed in [17]-[20]. It was noted that relatively less work has been reported for grid connected multiphase induction generator. Operation of grid connected induction generator (GCIG) is classified during fixed and variable speed of wind [21]. With fixed speed operation, fixing one set of stator winding, other winding set is manually adjusted avoid the mismatch of electrical and mechanical power [22]. On other hand, back to back power electronic converters decoupled with DC-link are employed for variable speed operation of induction generator. On machine side, multiple converters are used to supply the individual three-phase stator winding. Employed converters may be either connected in series enabling to boost up the DC link voltage [23], or in parallel connection for higher reliability and better efficiency [7], [24]. Owing for a successful operation of complete GCIG, various operational configurations are required to investigate in different modes. This paper proposes the two configurations of asymmetrical GCIG to fed the generated power through a single and double DC link circuit, interfaced with back to back converters.

In recent years, research attention has been diverted towards various intelligent optimization techniques, used in different engineering domains. Among the various techniques, PSO is

Manuscript received September 22, 2020; revised November 27, 2020; accepted December 14, 2020. date of publication March 25, 2021; date of current version March 18, 2021.

Arif Iqbal is with the Electrical Engineering Department, Rajkiya Engineering College Ambedkar Nagar, UP 224122, India (email: arif.iqbal.in@gmail.com).

Girish Kumar Singh is with the Electrical Engineering Department, Indian Institute of technology Roorkee, Uttarakhand 247667, India (email: gksngfee@gmail.com).

(Corresponding Author: Iqbal, Arif)

Digital Object Identifier 10.30941/CESTEMS.2021.00006

most popular algorithm based on nature-inspired metaheuristic optimization, originally developed by James Kennedy and Russell Eberhart in 1995 [25], [26], which conceptually simple, more robust towards parametric variation, computationally efficient and easy to implement. Utility of PSO has been also presented in wind power generation system particularly, control of pitch angle [27], rotor speed and tip-speed ratio [28] and, optimal design of wind farm [29]. However, through a detailed literature review, the authors of this paper are able to ascertain that the control of DC link voltage using PSO has not been reported so far. In this paper, complete research work may be formulated as:

a) Development of closed loop scheme using indirect field oriented control in two proposed configuration using single or double DC link circuit.
b) Tuning of PI controller parameters using PSO algorithm to ensure the flow of generated power to utility grid.
c) Experimental validation of control scheme and control of DC link voltage through the real time simulation on virtual platform.

II. Modeling of Six-Phase Induction Machine

Commonly three-phase stator winding of existing induction machine is reconfigured into six-phase (i.e. two sets of balanced winding, *abc* and *xyz*) by using the concept of phase belt split [4, 10]. During the reconfiguration process, asymmetry is ensured by having the phase shift of 30 degree between both three-phase winding sets *abc* and *xyz*. This is because, asymmetrical winding results the elimination of harmonics (lower order time and space harmonics) and hence a reduced torque pulsation for a smooth operation [4]-[8].

Considering ω as the speed of arbitrary reference frame, the voltage expression of asymmetrical six-phase induction machine is given as

$$\boldsymbol{v}_{qdk} = \boldsymbol{r}_{sk}\boldsymbol{i}_{qdk} + \frac{\omega}{\omega_b}\Phi_{dqk} + \frac{p}{\omega_b}\Phi_{qdk} \tag{1}$$

$$\boldsymbol{v}_{qdr} = \boldsymbol{r}_{qdr}\boldsymbol{i}_{qdr} + \left(\frac{\omega-\omega_r}{\omega_b}\right)\Phi_{dqr} + \frac{p}{\omega_b}\Phi_{qdr} \tag{2}$$

where, the terms used in the expression are defined in Appendix. Notation ϕ signifies the flux linkage per second in *d-q* frame which is related to the machine current, as given below

$$\Phi = \frac{\boldsymbol{X}}{\omega_b}\boldsymbol{i} \tag{3}$$

where, *X* is the reactance matrix

$$\boldsymbol{i} = \left[\left(\boldsymbol{i}_{qdk}\right)_{k=1,?2} \quad i_{qdr}\right]^T$$

$$\Phi = \left[\left(\Phi_{qdk}\right)_{k=1,?2} \quad \Phi_{qdr}\right]^T$$

With machine current as state variable, the voltage expressions can be conveniently written in matrix form

$$[v] = [z][i] \tag{4}$$

The electromagnetic torque, τ_e is given by:

$$\tau_e = c\sum_{k=1}^{2}\left(i_{qk}\Phi_{dk} - i_{dk}\Phi_{qk}\right) \tag{5}$$

$$\frac{\omega_r}{\omega_b} = \frac{1}{p}\left[\frac{1}{\omega_b}\frac{P}{2}\frac{1}{J}\left(\tau_e - \tau_l\right)\right] \tag{6}$$

where $c = \frac{3}{2}\frac{P}{2}\frac{1}{\omega_b}$, and all the symbols stand to their standard meaning.

III. Closed Loop Operation of Asymmetrical Six-Phase GCIG

For the high performance operation of induction machine (as generator), concept of indirect field oriented control is preferably used due to the decoupled control of torque and field component of current. It is achieved in closed loop operation of induction machine by developing a vector controller to obtain the suitable control switching signal to control the operation of machine side converters connected to both three-phase stator windings.

Machine voltage equation in synchronously rotating reference frame ($\omega_k = \omega_e$) is used to design a vector controller. Hence, rotor equation may be simplified as

$$0 = r_{qr}i_{qr} + \frac{\omega_{sl}}{\omega_b}\Phi_{dr} + \frac{p}{\omega_b}\Phi_{qr} \tag{7}$$

$$0 = r_{dr}i_{dr} - \frac{\omega_{sl}}{\omega_b}\Phi_{qr} + \frac{p}{\omega_b}\Phi_{dr} \tag{8}$$

where

$$\omega_{sl} = \omega_e - \omega_r \tag{8 A}$$

$$\Phi_{qr} = x_{lr}i_{qr} + x_m\left(i_{q1} + i_{q2} + i_{qr}\right) \tag{8 B}$$

$$\Phi_{dr} = x_{lr}i_{dr} + x_m\left(i_{d1} + i_{d2} + i_{dr}\right) \tag{8 C}$$

Considering rotor flux alignment along *d* axis, therefore

$$\Phi_r = \Phi_{dr} \tag{9}$$

$$\Phi_{qr} = 0 \tag{10}$$

$$\frac{p}{\omega_b}\Phi_r = 0 \tag{11}$$

Substitution of equations (9) – (11) into (7) and (8) yields,

$$r_{qr}i_{qr} + \frac{\omega_{sl}}{\omega_b}\Phi_r = 0 \tag{12}$$

$$r_{dr}i_{dr} + \frac{p}{\omega_b}\Phi_r = 0 \tag{13}$$

The value of i_{qr} and i_{dr} obtained from equation (8 B) – (8 C), substituted in equation (12) – (13) yield

$$\omega_{sl} = K_{sl}i_T \tag{14}$$

$$i_F = \left(1 + T_r\frac{p}{\omega_b}\right)\Phi_r \tag{15}$$

where

$$K_{sl} = \frac{x_m}{T_r\Phi_r} \tag{15 A}$$

$$i_T = i_{q1} + i_{q2} \tag{15 B}$$

$$i_F = i_{d1} + i_{d2} \tag{15 C}$$

$$T_r = \frac{(x_{lr} + x_m)}{\omega_b r_r} \quad (15\ D)$$

where, $T_r = \frac{(x_{lr} + x_m)}{\omega_b r_r}$ is rotor time constant.

The value of rotor current when substituted in torque equation will yield the following after simplification

$$\tau_e = K_T \Phi_r i_T = K_1 i_T \quad (16)$$

$$K_1 = K_T \Phi_r \quad (16\ A)$$

$$K_T = c \frac{x_m}{(x_{lr} + x_m)} \quad (16\ B)$$

The developed closed loop control strategy has been analytically investigated with its experimentally simulation in real time in two proposed configurations wherein, DC link voltage may be controlled by one and two grid connected converters as shown in Fig. 1 (a) and Fig 1 (b) respectively. The switching operation of machine side PWM converter has been synthesized by using the developed field oriented control, as shown in Fig. 2. During the implementation of scheme with wind turbine, MPPT block is used to obtain the optimized value of rotor speed as its reference value (ω_r^*) during the operation of GCIG in closed loop. A typical wind-speed characteristic of turbine used in the analysis is shown in Fig. 3 (a) and Fig. 3 (b).

IV. Control of Grid-side Converter

In this section, grid side converter (whose mathematically modeling is available in [30]) has been proposed to be controlled by using the concept of voltage oriented control [21]. This control is based on the transformation of stationary to synchronously rotating reference frame (i.e. *abc/dq* transformation) and vice-versa (i.e. *dq/abc* transformation) [3, 21]. During the transformation, grid side voltage angle θ_g is detected using the relation

$$\theta_g = tan^{-1}\left(\frac{v_\beta}{v_\alpha}\right) \quad (17)$$

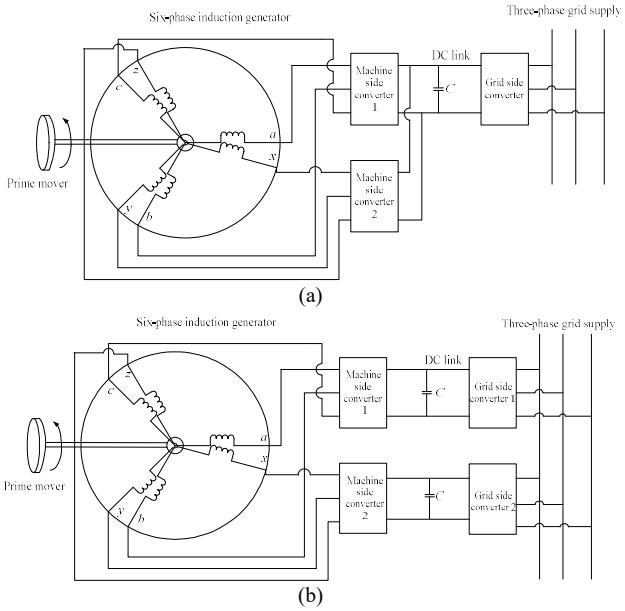

Fig. 1 Proposed configuration of six-phase GCIG with (a) one grid side converter (b) two grid side converter

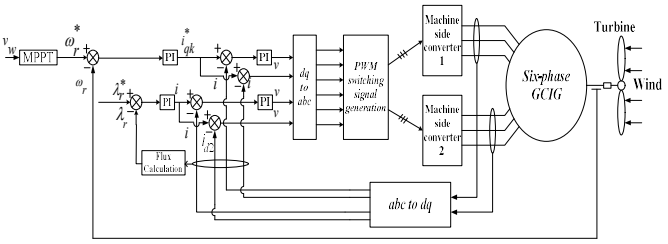

Fig. 2 Schematic representation of field oriented control of asymmetrical six-phase GCIG

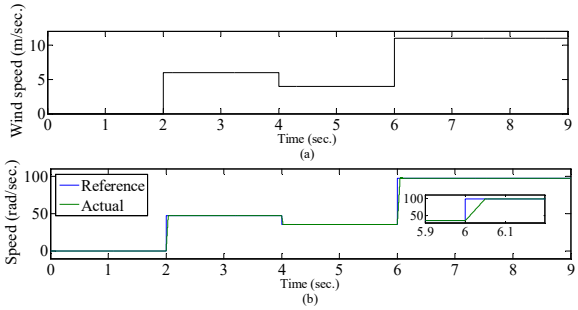

Fig. 3 Wind-speed characteristic of turbine

In the control scheme, the reference value of active current component is generated from DC link voltage error through proposed PSO based PI controller. Since the operation at unity power factor is considered, signifying the use of zero value for reactive component of current (i.e. $i_{dg}^* = 0$). Hence, after *dq/abc* transformation, reference grid currents (i_{ag}^* , i_{bg}^* , i_{cg}^*) are obtained which are further compared with its actual value(i_{ag} , i_{bg} , i_{cg}). After comparison, error signal is fed to a hysteresis controller to generate the switching signal (S_{ag} , S_{bg} , S_{cg}) on following logic

$$i_{jg} \le i_{jg}^* - \Delta i \text{ set } v_j = V_{dc} \quad (18)$$

$$i_{jg} \ge i_{jg}^* + \Delta i \text{ , reset } v_j = V_{dc} \quad (19)$$

where $j = a, b, c$

Value of Δi is taken as 0.0001 A. Complete implementation of grid side converter control has been depicted in Fig. 4.

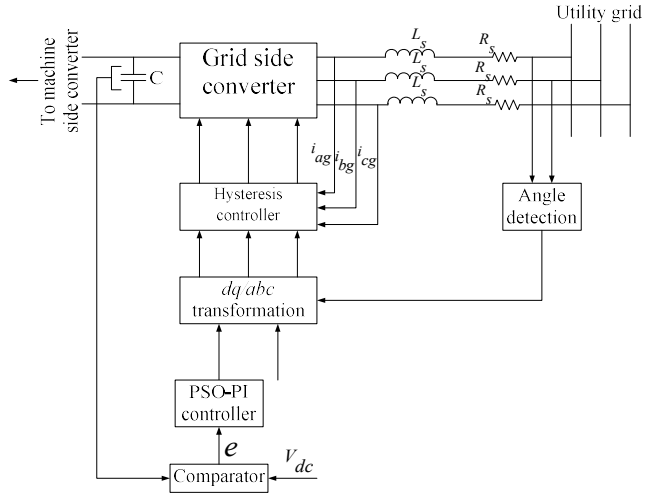

Fig. 4 Control scheme of grid side converter

V. Designing PI Controller Based on PSO Algorithm

In order to design PSO based system, swarm population of

size N in dimension D is considered whose position and velocity is given as

$$X_i = \left[X_{i,1}, X_{i,2}, \cdots, X_{i,D} \right] \quad (20)$$

$$V_i = \left[V_{i,1}, V_{i,2}, \cdots, V_{i,D} \right]; i = 1, 2, \cdots, N \quad (21)$$

Updated values of velocity and position of particles in iteration K are given as

$$V_i^{K+1} = W \times V_{i,j}^K + C_1 \times r_1 \left(P_{best\,i,j}^K - X_{i,j}^K \right) + C_2 \times r_2 \left(G_{best\,j}^K - X_{i,j}^K \right) \quad (22)$$

$$X_i^{K+1} = X_i^K + V_{i,j}^{K+1} \quad (23)$$

where $P_{best\,i,j}^K$ is personal best of i^{th} particle in j^{th} component and $G_{best\,j}^K$ is the global best (i.e. best individual) in j^{th} dimension of the population up to iteration K.

Above algorithm used to design a PI controller with two dimensional search spaces because two unknown values (i.e. K_p and K_i) are to be optimized. Complete step to implement the PSO algorithm to design PI controller for regulation of DC-link voltage is shown in Fig. 5

A. DC link voltage regulation

In the two proposed wind energy generation system, using one and two grid side converters are next investigated regarding DC link voltage regulation using PSO based PI controller. Here, PSO algorithm deals the design of an effective PI controller by determining the optimized value of two parameters, i.e. proportional and integral constants $(K_p \text{ and } K_i)$. For this purpose, the developed closed loop schemes were analytically implemented for 4 seconds. PSO parameters used during simulation are given Table I. Effectiveness of the proposed PSO based PI controller in both the suggested system configuration was accessed in comparison with conventional PI controller. It may be noted that cost function (CF) used during PSO algorithm implementation is given by

$$CF = minimize\left(\left(V_{dc} \right)_{reference} - \left(V_{dc} \right)_{actual} \right)^2 \quad (24)$$

In first system configuration with only one grid side converter, dynamic characteristic of proposed controller is shown in Fig. 6 (a) where, the initial DC link voltage at 550 V was increased to 650 V at time t=1.5sec It may be noted that proposed PSO based controller is reflecting a better performance both in terms of peak overshoot and settling time. A quantitative comparison between proposed and conventional controller is shown in Table II. Variation of cost function with respect to iteration count is shown in Fig. 6 (b). At the end of iteration, optimized value of controller parameters were found to be K_{p1}=0.74 and K_{i1}=4.9.

In second system configuration with two grid side converter, dynamic characteristic of proposed controller is shown in Fig. 7 (a). For simplicity, both the converters are assumed to be of same type. In this case the performance of proposed controller was also found to be superior than conventional PI controller, whose dynamic characteristic is shown in Fig. 7 (a). A quantitative comparison between proposed and conventional controller is also shown in Table III. Variation of cost function with respect to iteration count is shown in Fig. 7 (b). At the end of iteration, optimized value of controller parameters were found to be K_{p2}=0.64 and K_{i2}=2.97.

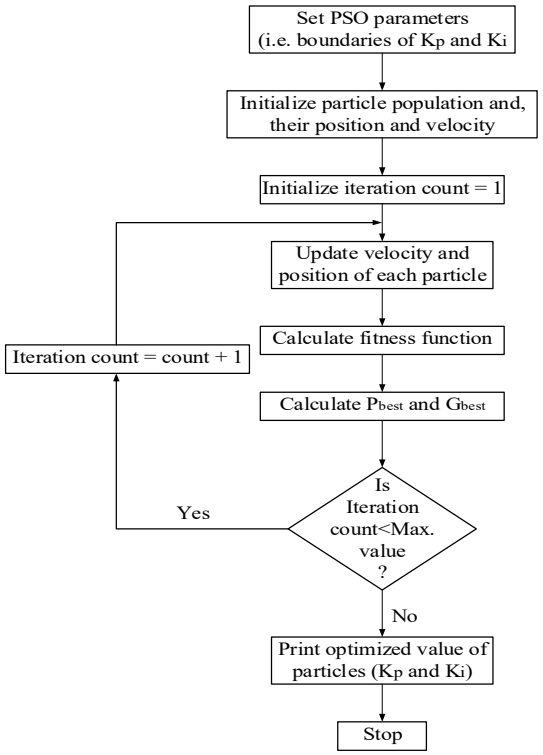

Fig. 5 Implementation steps to design PI controller based on PSO algorithm

TABLE I
PSO PARAMETERS

S. No.	Parameter	Value used
1.	Swarm size, N	4
2.	Inertia weight factor	0.9
3.	Confidence coefficient	2

TABLE II
PERFORMANCE COMPARISON OF PROPOSED AND CONVENTIONAL PI CONTROLLER IN FIRST SYSTEM CONFIGURATION

Time (sec.)	Controller type	Performance	
		Peak overshoot (V)	Settling time (sec.)
t = 0 (Starting)	PSO based	15	0.28
	Conventional PI	75	0.38
t = 1.5	PSO based	5.8	0.36
	Conventional PI	30	0.60

TABLE III
PERFORMANCE COMPARISON OF PROPOSED AND CONVENTIONAL PI CONTROLLER IN SECOND SYSTEM CONFIGURATION

Time (sec.)	Controller type	Performance	
		Peak overshoot (V)	Settling time (sec.)
t = 0 (Starting)	PSO based	69	0.46
	Conventional PI	137	0.62
t = 1.5	PSO based	6.0	0.48
	Conventional PI	38	0.74

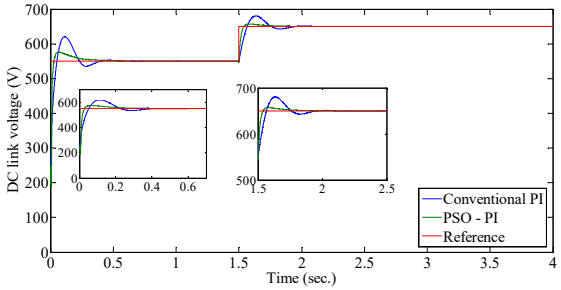

(a)

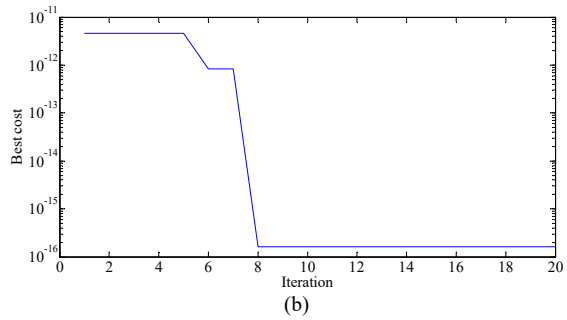

(b)

Fig. 6 Characteristic response of proposed PSO based PI controller in first system configuration showing (a) dynamic response (b) cost function with respect to algorithm iteration

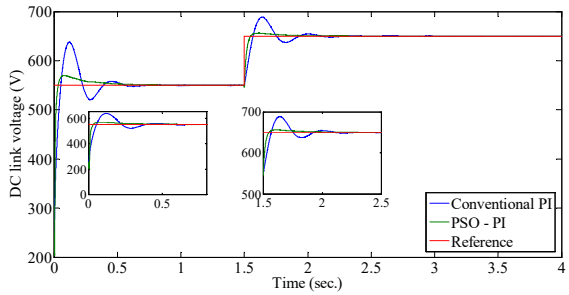

(a)

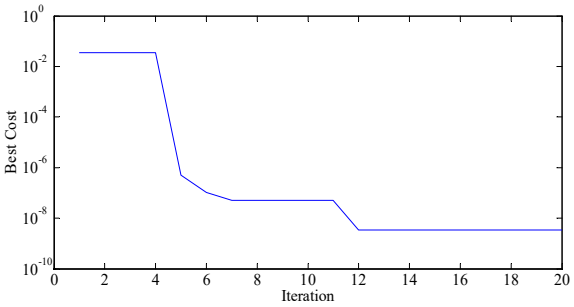

(b)

Fig. 7 Characteristic response of proposed PSO based PI controller in second system configuration showing (a) dynamic response (b) cost function with respect to algorithm iteration

VI. Analytical Results with its Validation

Usually the induction generator operates under variable wind speed in both the proposed generation system. It is to noted that the PI controller designed using PSO algorithm has been used here to regulate the DC link voltage (at 600 V) higher than the peak of grid voltage to ensure the flow of generated power from generator to utility grid.

A. Configuration I

At starting, the machine is allowed to run in motoring mode at rated speed under no load condition from time t = 0.2 sec. At time t = *2* sec., generation operation was initialized under the variation of wind speed, where rotor reference speed ω_r^* is obtained through MPPT. Complete rotor speed response is shown in Fig. 8 (a). It may be noted that DC link voltage was regulated at constant 600 V, irrespective to the variation in operational condition as shown in Fig. 8 (b). Since the generated power (active component of power) is transferred to utility grid hence, the active component of current associated with both stator winding sets, i_{q1} and i_{q2} was noted to be varied with respect to change in rotor speed, as shown in Fig. 9 (a) and Fig 9 (c) respectively. Variation reactive component of current i_{d1} and i_{d2} was not noted due to the consideration of constant flux operation of machine, shown in Fig. 9 (b) and Fig. 9 (d). All the analytical responses are further validated using experimental results virtually simulated in real time [31] using Typhoon HIL 402, as shown in Fig. 10 and Fig. 11. Close resemblance of results validating the correctness of analytical results.

B. Configuration II with reliability test

In this configuration, the operational conditions are same as discussed above. But, due to two separate use of grid side converters led the generation of two DC link voltages V_{dc1} and V_{dc2}. Magnitude of V_{dc1} and V_{dc2} is maintained constant at 600 V at different rotor speed. Response of rotor speed and DC link voltages i.e. ω_r, V_{dc1} and V_{dc2} is shown in Fig. 12 (a), Fig. 12 (b) and Fig. 12 (c) respectively. Current response associated with winding set *abc* and *xyz* i.e. i_{q1}, i_{d1}, i_{q2} and i_{d2} is shown in Fig. 13 (a), Fig. 13 (b), Fig. 13 (c) and Fig. 13 (d) respectively.

Furthermore, a reliability test on present system configuration was conducted during the occurrence of fault in one of the grid side converter at time t = 9 sec. Following to the outage of one converter, DC link voltage V_{dc2} becomes zero, as shown in Fig. 12 (c). Hence, the flow of power to utility grid associated with winding set *xyz* will be failed, signified by zero value of current i_{q2} and i_{d2} as shown in Fig. 13. But at the same time, continuity of power flow from generator through winding set *abc* is maintained with increased magnitude of current i_{q1} (by almost double), as shown in Fig. 13 (a).Hence, even during the outage of one grid side converter, the present system configuration II is capable to transfer the generated power to utility grid, emphasizing it to be used for reliable operation in

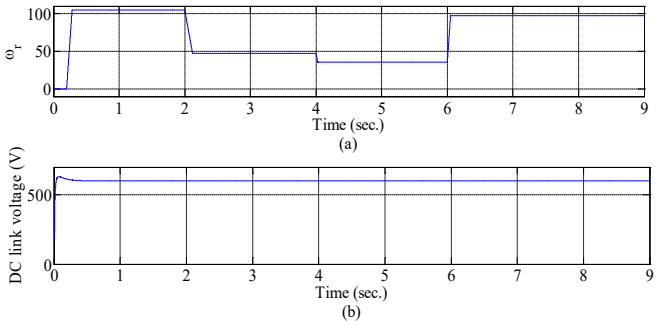

Fig. 8. Analytical results configuration I showing (a) rotor speed (b) DC link voltage

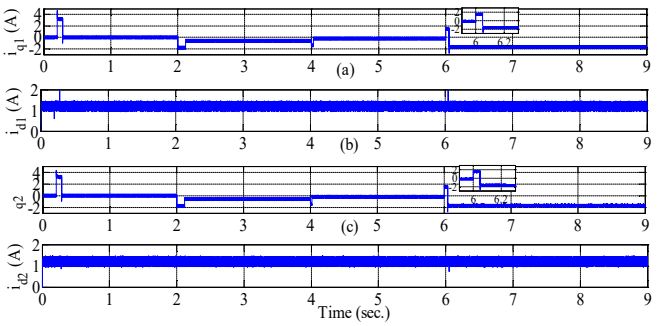

Fig. 9 Analytical results of configuration I showing *d-q* current (a) i_{q1} (b) i_{d1} (c) i_{q2} (d) i_{d2}

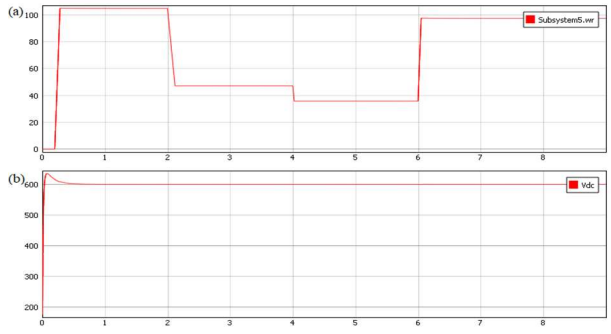

Fig. 10 Experimental simulation results in real time of configuration I showing (a) rotor speed (b) DC link voltage

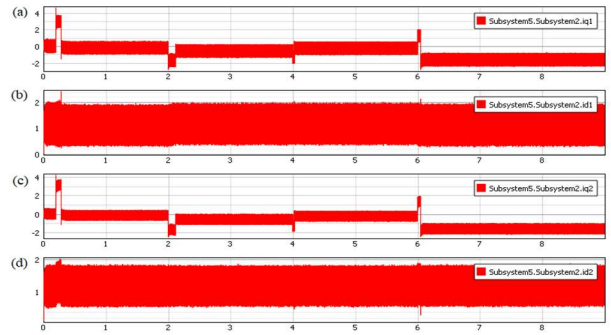

Fig. 11 Experimental simulation results in real time of configuration I showing *d-q* current (a) i_{q1} (b) i_{d1} (c) i_{q2} (d) i_{d2}

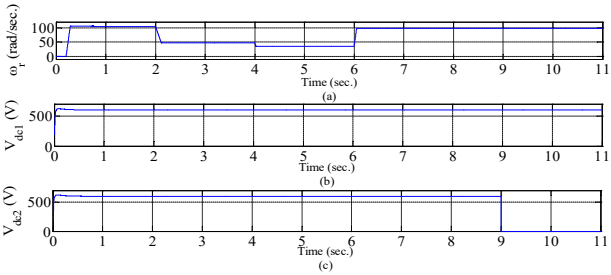

Fig. 12 Analytical results of configuration II showing (a) rotor speed (b) DC link voltage V_{dc1} (c) V_{dc2}

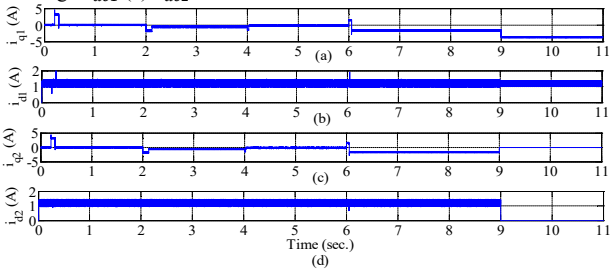

Fig. 13 Analytical results of configuration II showing *d-q* current (a) i_{q1} (b) i_{d1} (c) i_{q2} (d) i_{d2}

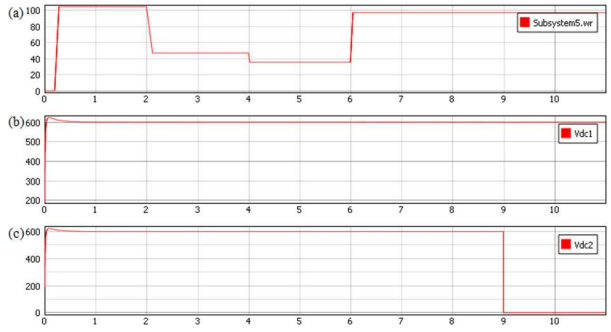

Fig. 14 Experimental simulation results in real time of configuration II showing (a) rotor speed (b) DC link voltage V_{dc1} (c) V_{dc2}

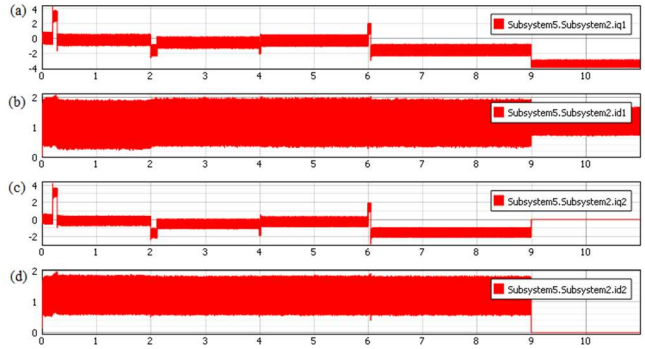

Fig. 15 Experimental simulation results in real time of configuration II showing *d-q* current (a) i_{q1} (b) i_{d1} (c) i_{q2} (d) i_{d2}

wind power generation system. It may be pointed here that the higher power rating grid side converter (more than machine rating) should be used to ensure a reliable operation of proposed system configuration. The analytical results shown in Fig. 12 and Fig. 13 have been completely verified through experimental simulation in real time on virtual platform, as shown in Fig. 14 and Fig. 15. Close resemblance of results validating the correctness of analytical results.

VII. Experimental Results

The developed system in closed loop operation with indirect field oriented control was also experimentally implemented on a test rig, as shown in Fig. 16. In this setup, configuration I was used for experimental investigation. During implementation, two level converters were used where the switching signals of SEMIKRON IGBT were obtained through dSPACE (DS1104). On generator side, optimized rotor reference speed was obtained through MPPT algorithm and, an independent variation in stator current was noted with winding sets *abc* and *xyz*, as shown in Fig. 17 (a) and Fig. 17 (b) respectively. Variation in *d*-component current i_{d1} and i_{d2} was not noted because the constant flux operation was considered. Negative value of *q*-component current i_{q1} and i_{q2} indicates the flow of active power from generator to utility grid. It may be noted here that during the transient period, current i_{q1} and i_{q2} shoots to positive value. This may be accounted with the fact that the reference rotor speed changes through MPPT due to change in wind speed and to extract the maximum power, machine operates as motor with positive value of *q*-component current. This phenomenon has been also shown in simulation results in above section for both the proposed configurations. Throughout the implementation, the DC link voltage is maintained constant at 600 V (higher than the peak grid voltage) as shown in Fig. 18 (a). This ensures flow of generated power to utility grid at unity power factor (pf), as shown in the voltage and current waveform in Fig. 18 (b) and Fig. 18 (c) respectively. Together with the pf, other performance indices are shown in Fig. 18 (d). In this figure, the unity pf with negative value is showing the feeding of power to utility grid. During experiment, it was assumed that wind speed is 11 m/sec, and generated power is 630 W which is fed to grid. The similarity of experimental responses may be noted with both analytical and real time simulation results.

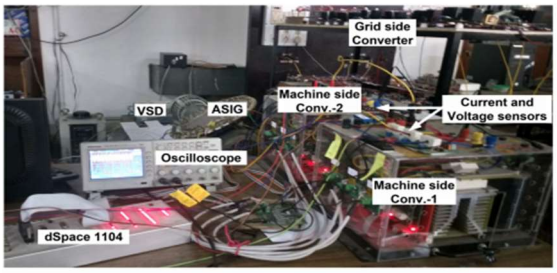

Fig. 16: Experimental setup showing various used equipments

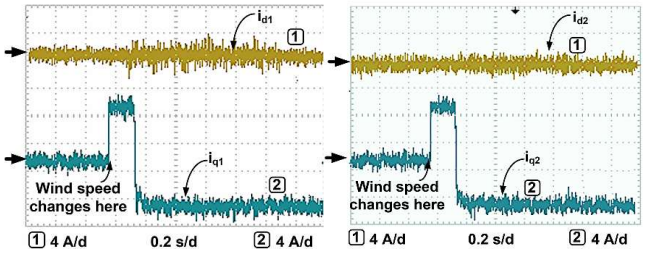

(a) (b)

Fig. 17: *d-q* component of stator current of (a) winding set *abc* and (b) winding set *xyz*

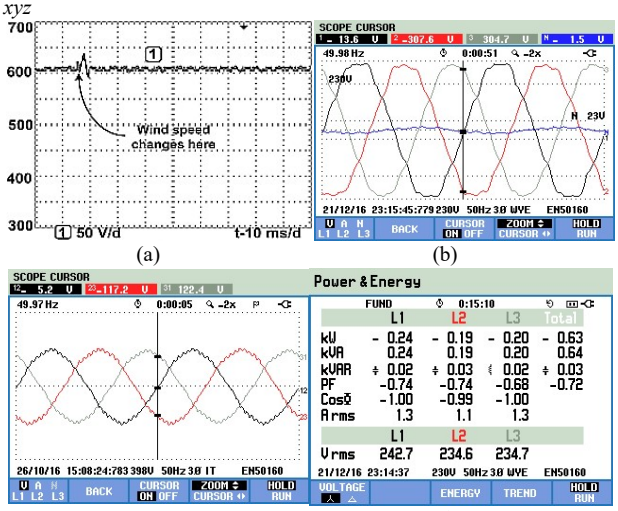

(a) (b) (c) (d)

Fig. 18: Experimental waveforms showing (a) dc-link voltage (b) grid voltage (c) grid current (d) performances indices

VIII. CONCLUSION

This paper proposes the design of an advanced auto-tuned PI controller based on PSO algorithm to regulate the DC link voltage at constant 600 V (higher than the peak grid voltage). This is to ensure the flow of generated power to utility grid. Performance of PSO based PI controller was found to be better in comparison with conventional controller particularly, in terms of peak over shoot and settling time.

Furthermore, the two configurations of complete wind power generation system have been proposed. In configuration I, only one DC link circuit was used with one grid side converter whereas, in configuration II has two DC link circuits with two grid side converters. Both the proposed configurations have been extensively investigated analytically under variable wind speed. Analytical results have been validated through experimental results through real time simulation on virtual platform. During the performance evaluation, configuration II has been proposed to be used where reliability is of prime importance. This is because, during the outage of one grid side converter, GCIG is still capable to supply the power through one remaining healthy grid side converter. Key analytical results have been further tested and validated on a test rig.

Present analysis (both theoretical and experimental) may be investigated further to more number of phases in machine stator (like 9, 12, 15 etc. phase machine) as well as grid connected multiphase multi-machine system.

APPENDIX

PARAMETERS OF 1.1 kW, SIX-PHASE, SIX POLES, 36 SLOTS, 50 Hz. INDUCTION MACHINE

$r_1 = 4.12\ \Omega$	$r_2 = 4.12\ \Omega$	$r_r = 8.79\ \Omega$
L_{lr} =21.6 mH	$L_m = 234.6\ mH$	$L_{ldq} = 0\ H$
$L_{l1} = L_{l2} = 21.6\ mH$	$L_{lm} = 0.002\ H$	J=0.089 Kgm^2

$$\boldsymbol{v}_{\boldsymbol{qdk}} = \begin{bmatrix} v_{qk} & v_{dk} \end{bmatrix}^T ;\ \boldsymbol{v}_{\boldsymbol{qdr}} = \begin{bmatrix} v_{qr} & v_{dr} \end{bmatrix}^T$$

$$\Phi_{\boldsymbol{qdk}} = \begin{bmatrix} \Phi_{qk} & \Phi_{dk} \end{bmatrix}^T ; \Phi_{\boldsymbol{dqk}} = \begin{bmatrix} \Phi_{dk} & -\Phi_{qk} \end{bmatrix}^T$$

$$\Phi_{\boldsymbol{qdr}} = \begin{bmatrix} \Phi_{qr} & \Phi_{dr} \end{bmatrix}^T ;\ \Phi_{\boldsymbol{dqr}} = \begin{bmatrix} \Phi_{dr} & -\Phi_{qr} \end{bmatrix}^T$$

$$\boldsymbol{i}_{\boldsymbol{qdk}} = \begin{bmatrix} i_{qk} & i_{dk} \end{bmatrix}^T ;\ \boldsymbol{i}_{\boldsymbol{qdr}} = \begin{bmatrix} i_{qr} & i_{dr} \end{bmatrix}^T$$

$$\boldsymbol{v} = \begin{bmatrix} \left(\boldsymbol{v}_{\boldsymbol{qdk}}\right)_{k=1,2} & \boldsymbol{v}_{\boldsymbol{qdr}} \end{bmatrix}^T ; \boldsymbol{i} = \begin{bmatrix} \left(\boldsymbol{i}_{\boldsymbol{qdk}}\right)_{k=1,2} & \boldsymbol{i}_{\boldsymbol{qdr}} \end{bmatrix}^T$$

where,

$$k = \begin{cases} 1, \textit{ for winding set abc} \\ 2, \textit{ for winding set xyz} \end{cases}$$

$$z = \begin{bmatrix}
r_1 + \frac{p}{\omega_b}\left(x_{l1} + x_{lm} + x_m\right) & \frac{\omega_e}{\omega_b}\left(x_{l1} + x_{lm} + x_m\right) & \frac{p}{\omega_b}\left(x_{lm} + x_m\right) & \frac{\omega_e}{\omega_b}\left(x_{lm} + x_m\right) & \frac{p}{\omega_b}x_m & \frac{\omega_e}{\omega_b}x_m \\
-\frac{\omega_e}{\omega_b}\left(x_{l1} + x_{lm} + x_m\right) & r_1 + \frac{p}{\omega_b}\left(x_{l1} + x_{lm} + x_m\right) & -\frac{\omega_e}{\omega_b}\left(x_{lm} + x_m\right) & \frac{p}{\omega_b}\left(x_{lm} + x_m\right) & -\frac{\omega_e}{\omega_b}x_m & \frac{p}{\omega_b}x_m \\
\frac{p}{\omega_b}\left(x_{lm} + x_m\right) & \frac{\omega_e}{\omega_b}\left(x_{lm} + x_m\right) & r_2 + \frac{p}{\omega_b}\left(x_{l2} + x_{lm} + x_m\right) & \frac{\omega_e}{\omega_b}\left(x_{lm} + x_m\right) & \frac{p}{\omega_b}\left(x_{lm} + x_m\right) & \frac{\omega_e}{\omega_b}x_m \\
-\frac{\omega_e}{\omega_b}\left(x_{lm} + x_m\right) & \frac{p}{\omega_b}\left(x_{lm} + x_m\right) & -\frac{\omega_e}{\omega_b}\left(x_{lm} + x_m\right) & r_2 + \frac{p}{\omega_b}\left(x_{l2} + x_{lm} + x_m\right) & -\frac{\omega_e}{\omega_b}x_m & \frac{p}{\omega_b}x_m \\
\frac{p}{\omega_b}x_m & \frac{s\omega_e}{\omega_b}x_m & \frac{p}{\omega_b}x_m & \frac{s\omega_e}{\omega_b}x_m & r_r + \frac{p}{\omega_b}\left(x_{lr} + x_m\right) & \frac{s\omega_e}{\omega_b}\left(x_{lr} + x_m\right) \\
-\frac{s\omega_e}{\omega_b}x_m & \frac{p}{\omega_b}x_m & \frac{p}{\omega_b}x_m & \frac{p}{\omega_b}x_m & -\frac{s\omega_e}{\omega_b}\left(x_{lr} + x_m\right) & r_r + \frac{p}{\omega_b}\left(x_{lr} + x_m\right)
\end{bmatrix}$$

$$X=\begin{bmatrix} (x_{l1}+x_{lm}+x_m) & 0 & (x_{lm}+x_m) & 0 & x_m & 0 \\ 0 & (x_{l1}+x_{lm}+x_m) & 0 & (x_{lm}+x_m) & 0 & x_m \\ (x_{lm}+x_m) & 0 & (x_{l2}+x_{lm}+x_m) & 0 & x_m & 0 \\ 0 & (x_{lm}+x_m) & 0 & (x_{l2}+x_{lm}+x_m) & 0 & x_m \\ x_m & 0 & x_m & 0 & (x_{lr}+x_m) & 0 \\ 0 & x_m & 0 & x_m & 0 & (x_{lr}+x_m) \end{bmatrix}$$

REFERENCES

[1] https://www.irena.org/wind

[2] https://gwec.net/global-figures/wind-energy-global-status

[3] Bose BK (2002) *Modern power electronics and AC drives*, NJ, Upper Saddle River, Prentice Hall, Inc.

[4] G. K. Singh, "Multi-phase induction machine drive research-a survey", *Electric Power System Research*, vol. 61, no. 2, pp. 139–147, Mar. 2002. DOI: 10.1016/S0378-7796(02)00007-X

[5] K. A. Chinmaya, and G. K. Singh, "Performance evaluation of multiphase induction generator in stand-alone and grid connected wind energy conversion system", *IET Renewable Power Generation*, vol. 12, no. (7), pp. 823-831, May 2018. DOI: 10.1049/iet-rpg.2017.0791

[6] A. Iqbal, G. K. Singh, and V. Pant, "Stability analysis of an asymmetrical six-phase synchronous motor", *Turkish Journal of Electrical Engineering & Computer Science*, vol. 34, no. 3, pp. 1674–1692, Mar. 2016. DOI:10.3906/elk-1403-46

[7] A. Iqbal, and G. K. Singh, "Eigenvalue analysis of six-phase synchronous motor for small signal stability", *European Power Electronics Journal*, vol. 28, no. 2, pp. 49-62, Jan. 2018. DOI:10.1080/09398368.2018.1425241

[8] G. K. Singh, and A. Iqbal, "Small Signal Stability of Three-phase and Six-phase Synchronous Motors: A Comparative Analysis", *Chinese Journal of Electrical Engineering*, vol. 6, no. 1, pp. 22-40, Apr. 2020. DOI: 10.23919/CJEE.2020.000002

[9] K.A. Chinmaya and G.K. Singh, "Modeling and experimental analysis of grid-connected six-phase induction generator for variable speed wind energy conversion system", *Electric Power Systems Research*, vol. 166, pp. 151-162, Jan. 2019. DOI: 10.1016/j.epsr.2018.10.007

[10] E. A. Klingshirn, "High Phase Order Induction Motors - Part I-Description and Theoretical Considerations. *IEEE Transaction on Power Apparatus & System*, vol. 3, no. 1, pp. 47-53, Jan. 1983. DOI: 10.1109/MPER.1983.5519568

[11] G. K. Singh, "Modeling and experimental analysis of a self-excited six-phase induction generator for stand-alone renewable energy generation", *Renewable Energy*, vol. 33, no. 7, pp. 1605–1621, July 2008. DOI: 10.1016/j.renene.2007.08.007

[12] G. K. Singh, A. S. Kumar, and R. P. Saini, "Steady-state modeling and analysis of six-phase self-excited induction generator for renewable energy generation", *Electric Power Component & Systems*, vol. 38, no. 2, pp. 137–151, Dec. 2009. DOI: 10.1080/15325000903273346

[13] G. K. Singh, A. S. Kumar, and R. P. Saini, "Selection of capacitance for self-excited six-phase induction generator for stand-alone renewable energy generation", *Energy*, vol. 35, no. 8, pp. 3273–3283, Aug. 2010. DOI: 10.1016/j.energy.2010.04.012

[14] M. F. Khan, M. R. Khan and A. Iqbal, "Modeling, implementation and analysis of a high (six) phase self-excited induction generator", Journal of Electrical Systems and Information Technology, vol. 5, no. 3, pp. 794-812, Dec. 2018. DOI: 10.1016/j.jesit.2016.12.016

[15] G. K. Singh, A. S. Kumar, and R. P. Saini, "Performance analysis of a simple shunt and series compensated six-phase self-excited induction generator for stand-alone renewable energy generation", *Energy Conversion & Management*, vol. 52, no. 3, pp. 1688–1699, Mar. 2011. DOI: 10.1016/j.enconman.2010.10.032

[16] G. K. Singh, A. S. Kumar, and R. P. Saini, "Performance evaluation of series compensated self-excited six-phase induction generator for stand-alone renewable energy generation", *Energy*, vol. 35, no. 1, pp. 288–297, Jan. 2010. DOI: 10.1016/j.energy.2009.09.021

[17] O. Ojo, and I. E. Davidson, "Pwm-vsi inverter-assisted stand-alone dual stator winding induction generator", *IEEE Transaction on Industrial Applications*, vol. 36, no. 6, pp. 1604–1611, Nov./Dec. 2000. DOI: 10.1109/IAS.1999.805950

[18] Z. Wu, O. Ojo, and J. Sastry, "High-performance control of a dual stator winding dc power induction generator", *IEEE Transaction on Industrial Applications*, vol. 43, no. 2, pp. 582–592, Mar. 2007. DOI:10.1109/TIA.2006.890020

[19] Y. Li, Y. Hu, W. Huang, L. Liu and Y. Zhang, "The capacity optimization for the static excitation controller of the dual-stator-winding induction generator operating in a wide speed range", *IEEE Transaction on Industrial Electronics*, vol. 56, no. 2, pp. 530–541, Feb. 2009. DOI: 10.1109/TIE.2008.2003363

[20] M. Moradian, and J. Soltani, "An isolated three-phase induction generator system with dual stator winding sets under unbalanced load condition", *IEEE Transaction on Energy Conversion*, vol. 31, no. 2, pp. 531–539, Jan. 2016. DOI: 10.1109/TEC.2015.2508958

[21] B. Wu, Y. Lang, N. Zargari, and S. Kouro, "Power conversion and control of wind energy systems. *John Wiley & Sons*, New Jersey, 2011.

[22] D. Levy, "Analysis of a double-stator induction machine used for a variable speed/constant-frequency small-scale hydro/wind electric power generator", *Electric Power System Research*, vol. 11, no. 3, pp. 205–223, Dec. 1986. DOI:10.1016/0378-7796(86)90035-0

[23] H. S. Che, E. Levi, M. Jones, M. J. Duran, H. Hew, and N. A. Rahim, " Operation of a six-phase induction machine using series-connected machine-side converters", *IEEE Transaction on Industrial Electronics*, vol. 61, no. 1, pp. 164–176, Feb. 2013. DOI:10.1109/TIE.2013.2248338

[24] J. A. B. Rodrigo, J. I. Talpone, and L. M. Salamero, "Variable-speed wind energy conversion system based on a dual stator-winding induction generator", *IET Renewable Power Generation*, vol. 11, no. 1, pp. 73–80, Apr. 2017. DOI: 10.1049/iet-rpg.2016.0186

[25] Kennedy J, and Eberhart R, "Particle swarm optimization", *IEEE International Conference on Neural Networks*, 1995, pp. 1942-1948. DOI: 10.1109/ICNN.1995.488968

[26] Eberhart R, and Kennedy J, "A new optimizer using particle swarm theory", *IEEE Proceedings of the Sixth International Symposium on Micro Machine and Human Science*, 1995, pp. 39-43. DOI: 10.1109/MHS.1995.494215

[27] M. B. Smida, and A. Sakly, "Smoothing wind power fluctuations byparticle swarm optimization-based pitch angle controller", *Transactions of the Institute of Measurement and Control*, vol. 41, no. 3, pp. 647-656, May 2018. DOI: 10.1177/0142331218764594

[28] C. Kongnam, and S. Nuchprayoon, "A particle swarm optimization for wind energy control problem", *Renewable Energy*, vol. 35, no. 11, pp. 2431-2438, Nov. 2010. DOI: 10.1016/j.renene.2010.02.020

[29] V. Aristidis, P. Maria, and L. Christos, "Particle Swarm Optimization (PSO) algorithm for windfarm optimal design", *International Journal of Management Science and Engineering Management*, vol. 5, no. 1, pp. 53-58, May 2013. DOI: 10.1080/17509653.2010.10671091

[30] V. F. Pires, and J. F. Silva, "Teaching nonlinear modeling, simulation, and control of electronic power converter using MATLAB/SIMULINK", *IEEE Transaction on Education*, vol. 45, no. 3, pp. 253-261, Aug. 2002. DOI: 10.1109/TE.2002.1024618

[31] F. Li, Y. Wang, F. Wu, Y. Huang, Y. Liu, X. Zhang, and M. Ma, "Review of Real-time Simulation of Power Electronics. *Journal of Modern Power Systems and Clean Energy*, vol. 8, no. 4, pp. 796-808, Jul. 2020. DOI: 10.35833/MPCE.2018.000560

Arif Iqbal received his B.Tech. and M.Tech. degrees both in Electrical Engineering, from Aligarh Muslim University, Aligarh, India, in 2005 and 2007, respectively. He has completed his Ph.D. from Indian Institute of Technology, Roorkee, India, in 2015. He is having an experience of four years in industry and teaching in the field AC drives and power system. Currently, he is working as Assistant Professor in the Electrical Engineering Department, Rajkiya Engineering College Ambedkar Nagar, Akbarpur, India. His area of interest is multiphase AC machine & drives, power electronics and renewable energy system.

Girish Kumar Singh received the B.Tech. degree in Electrical Engineering from G. B. Pant University of Agriculture and Technology, Pantnagar, India, in 1981, and the Ph.D. degree in electrical engineering from Banaras Hindu University, Varanasi, India, in 1991. He worked in the industry for nearly five-and-a half years. In 1991, he became a Lecturer at M.N.R. Engineering College, Allahabad, India. In 1996, he moved to University of Roorkee, Roorkee, India. Currently, he is Professor in Electrical Engineering Department, Indian Institute of Technology, Roorkee. He has been involved in the design and analysis of electrical machines in general and high-phase-order ac machines in particular as well as power system harmonics and power quality. He has coordinated a number of research projects sponsored by the CSIR and UGC, Government of India. He has also coordinated a research project sponsored by University of Malaya, Govt. of Malaysia. Dr. Singh has served as Visiting Professor, Department of Electrical Engineering, University of Malaya, Malaysia w.e.f July 29, 2013 to July 28, 2014 and as Visiting Professor in Department of Electrical and Electronics Engineering, Middle East Technical University, Ankara, Turkey from December 27, 2006 to June 27, 2007. He has also served as Visiting Associate Professor in Department of Electrical Engineering from June 28, 2003 to December 24, 2003, Pohang University of Science and Technology, South Korea. Prof. Singh received the Pt. Madan Mohan Malaviya Memorial Medal and the Certificate of Merit Award 2001–2002 at The Institution of Engineers (India).